Temperature dependence of irradiation-induced amorphization in a high-entropy titanate pyrochlore

William J. Weber[a*], Candice Kinsler-Fedon[a], Veerle Keppens[a], Yanwen Zhang[a,b], Anamul H. Mir[c]

[a]Department of Materials Science & Engineering, University of Tennessee, Knoxville, Tennessee 37996, USA

[b]Department of Mechanical & Materials Engineering, Queen's University, Kingston, ON K7L 3N6, Canada

[c]School of Computing & Engineering, University of Huddersfield, Huddersfield HD1 3DH, UK

Corresponding author(s) email: *wjweber@utk.edu

Abstract

The temperature dependence of amorphization in a high-entropy pyrochlore, $(Yb_{0.2}Tm_{0.2}Lu_{0.2}Ho_{0.2}Er_{0.2})_2Ti_2O_7$, under irradiation with 600 keV Xe ions has been studied using in-situ transmission electron microscopy (TEM). The critical amorphization dose increases with temperature, and the critical temperature for amorphization is 800 K. At room temperature, the critical amorphization dose is larger than that previously determined for this pyrochlore under bulk-like 4 MeV Au ion irradiation but is similar to the critical doses determined in two other high-entropy titanate pyrochlores under 800 keV Kr ion irradiation using in-situ TEM, which is consistent with reported behavior in simple rare-earth titanate pyrochlores.

KEYWORDS: ceramic, ion-solid interactions, phase transformation, radiation effects, transmission electron microscopy (TEM)

Introduction

The advancement of high-entropy oxides (HEOs), with 5 or more elements on a cation site, has ushered in a new realm of complexity and flexibility in the tunability of functionalities in advanced technical oxides for electro-optical, magnetic, ionic transport and nuclear applications. Many structure types of HEOs have been formed by solid-state reactions and characterized [1,2], and HEOs with the pyrochlore structure ($A_2B_2O_7$) have been synthesized with multiple elements on either the A-site [3,4] or B-site [5,6], as well as on both A- and B-sites [7]. The flexibility and phase stability of the cubic HEO pyrochlore structure allow a range of compositions that can be tuned to create unique properties and functionalities, including exotic magnetic properties [4], low thermal diffusivity [3,5], improved mechanical properties [6], high ionic conductivity [8], and radiation tolerance [7,9].

Ion-beam modification is widely used to tune the properties, structure, and functionality of many types of ceramic oxides [10], but data on HEOs are limited. While HEO pyrochlores have been suggested as matrices for immobilization of nuclear waste [7,11], studies on the radiation behavior and kinetics are also limited. One of the first studies on the response of HEOs to ion-beam irradiation has been conducted on a single crystal titanate pyrochlore, $(Yb_{0.2}Tm_{0.2}Lu_{0.2}Ho_{0.2}Er_{0.2})_2Ti_2O_7$, aligned along the [100] direction, and Rutherford backscattering spectrometry in channeling geometry (RBS/C) has been employed to follow the dependence of irradiation-induced amorphization on dose due to irradiation with 4 MeV Au ions at room temperature [12,13]. Raman spectroscopy has been used to follow irradiation-induced amorphization in single crystal $(Yb_{0.2}Tb_{0.2}Gd_{0.2}Dy_{0.2}Er_{0.2})_2Ti_2O_7$ pyrochlore irradiated at room temperature with 23 MeV Ni ions [13]. Both grazing incident x-ray diffraction and Raman spectroscopy have been applied to study irradiation-induced amorphization in polycrystalline $(Gd_{0.2}Dy_{0.2}Ho_{0.2}Er_{0.2}Yb_{0.2})_2Ti_2O_7$ and $(Gd_{1/6}Dy_{1/6}Er_{1/6}Yb_{1/6}Ho_{1/6}Nd_{1/6})_2Ti_2O_7$ pyrochlores irradiated with 3 MeV Au ions at room temperature [14]. Other studies of irradiation-induced amorphization have been carried out on polycrystalline $(Lu_{0.25}Y_{0.25}Eu_{0.25}Gd_{0.25})_2Ti_2O_7$ [15] and $(Lu_{0.2}Y_{0.2}Gd_{0.2}Eu_{0.2}Sm_{0.2})_2Ti_2O_7$ [16] pyrochlores using in-situ transmission electron microscopy (TEM) with 800 keV Kr ions at room temperature. Such in-situ TEM approaches follow the ion irradiation of electron-transparent thin regions in a sample.

All irradiation studies to date on pyrochlores samples have been conducted at room temperature. In this work, we report the results of an in-situ TEM irradiation study of the previously studied $(Yb_{0.2}Tm_{0.2}Lu_{0.2}Ho_{0.2}Er_{0.2})_2Ti_2O_7$ single crystal, but over a broad range of temperatures to evaluate the temperature dependence and to determine the critical temperature for amorphization (i.e., temperature above which full amorphization does not occur for a given ion species and energy). In addition, the critical dose, D_c, for amorphization at room temperature in high-entropy and simple titanate pyrochlores under different ion irradiation conditions is compared and discussed.

Materials and Methods

The single crystal $(Yb_{0.2}Tm_{0.2}Lu_{0.2}Ho_{0.2}Er_{0.2})_2Ti_2O_7$ used in this study and a previous study [12,13] was grown using the floating-zone growth technique and a two-mirror optical floating-zone furnace (Canon Machinery model SC1-MDH) with 1500-W halogen lamps. This crystal growth procedure used oxygen atmosphere at a pressure of 0.2 MPa and a growth rate of 5-6 mm per hour. A section of the crystal was crushed for TEM specimen preparation, and a small amount of the crushed HEO pyrochlore was placed in a mortar and mixed with ethanol. A small amount of the suspension (containing ethanol and HEO pyrochlore grains) was deposited onto TEM grids covered with holey carbon film. Only HEO grains found at the edge of the holes and having similar thicknesses were characterized to avoid diffraction data coming from the amorphous carbon film.

Transmission electron microscopy (TEM) analysis under in-situ Xe ion irradiation was performed at the MIAMI-2 facility in Huddersfield, UK [17]. The TEM analysis was carried out on a Hitachi H-9500 TEM (300 keV) equipped with Gatan Model 963 GIF (Gatan Imaging Filter), which allowed Energy Filtered Transmission Electron Microscopy (EF-TEM) images to be taken and determinations of the HEO pyrochlore grain thickness to be made. The inelastic mean free path (λ) in pyrochlore for 300 keV electrons is 120 nm, which was calculated using information and methodologies reported previously [18,19].

In-situ ion irradiations with 600 keV Xe^{2+} were carried out with a 350 kV National Electrostatics Corporation ion accelerator connected to the electron microscope [17]. The irradiations were performed at an incident angle of 2 to 5 degrees from the sample normal by tilting the TEM holder towards the ion beam with ion fluxes between 2×10^{12} to 3.5×10^{12} ions $cm^{-2}s^{-1}$ for the various experiments conducted for the determination of critical amorphization fluence (ion beam monitoring and dosimetry at the MIAMI-2 facility are discussed in detail elsewhere [17]). The electron beam was turned off during the ion irradiation and switched on only for a few seconds (less than 5 s) when capturing the selected area electron diffraction (SAED) patterns between the ion irradiation steps. The irradiations were repeated at each temperature until the HEO pyrochlore became completely amorphous (when no diffraction spots were visible). The irradiations and subsequent TEM analysis were conducted at temperatures of 143 K, 200 K, 298 K, 483 K, 683 K, 723 K, 753 K, 783 K, 883 K, 983 K and 1073 K. The range of fluences increased with temperature, up to a maximum fluence of 6.03×10^{15} ions cm^{-2} at 1073 K. The SAED images were processed with the DigitalMicrograph, Fiji DiffTools [20] and SingleCrystalTM software (www.crystalmaker.com).

The Stopping and Range of Ions in Matter code (SRIM-2013) [21] was used to determine the ion ranges and depth profile of damage production for the 600 keV Xe ions in the HEO pyrochlore, as well as the depth profiles of electronic energy loss (S_e) and nuclear energy loss (S_n). As in the previous study on this HEO pyrochlore [12], the simulations were performed in full-cascade mode [22], assuming a threshold

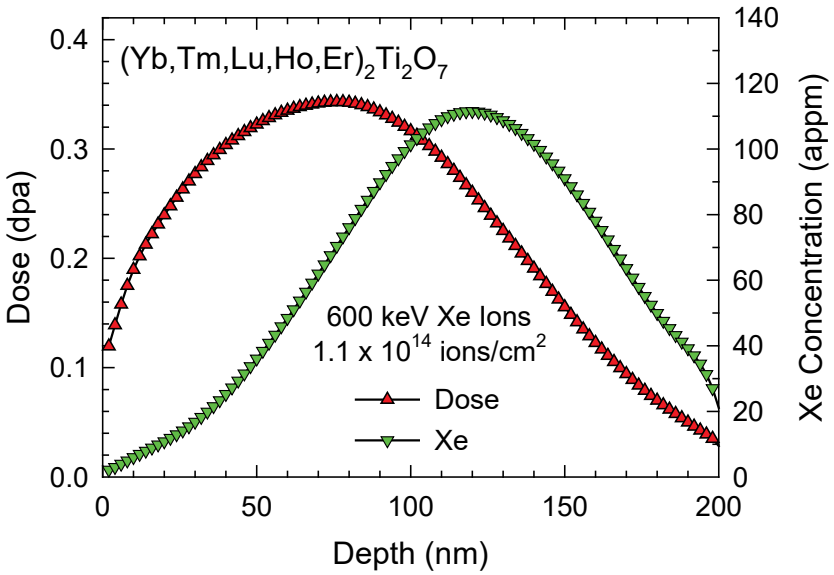

Figure 1. The depth profiles of local damage dose (dpa) and implanted Xe concentration (appm) for an ion fluence of 1.1 x 10^{14} (critical amorphization fluence at 298 K).

displacement energy of 50 eV for each element in the HEO pyrochlore and an experimentally derived density of 7 g/cm^3. All comparisons to other HEO and simple pyrochlores in this work are based on similar SRIM simulations of damage production assuming a threshold displacement energy of 50 eV for all elements and the appropriate density for each compound. In this work, the depth dependent damage dose in displacements per atom (dpa) was determined at each fluence for full amorphization, and the damage dose assigned for full amorphization was that at a depth of 30 nm, as in previous in-situ TEM studies on pyrochlores [23].

Results

The depth profiles of local damage dose (dpa) and implanted Xe concentration (appm) at a fluence of 1.1 $\times 10^{14}$ ions/cm^2 (the amorphization fluence at 298 K) are shown in Fig. 1. Analyzed regions in the TEM specimens were selected to be about 70 nm thick; thus, the Xe concentration is less than several hundred appm, even at the highest fluence of 6.03 $\times$ 10^{15} ions/cm^2.

A bright-field TEM image of the specimen irradiated at 298 K is shown in Fig. 2 (a), and an EF-TEM thickness map of the specimen is provided in Fig. 2 (b), with the corresponding histogram in Fig. 2 (c). The region labeled 1 in Fig. 2 (a) is where the SAED analysis was conducted after each fluence in this specimen and has mean thickness of about 70 nm based on the inelastic mean free path (λ) of 120 nm for 300 keV

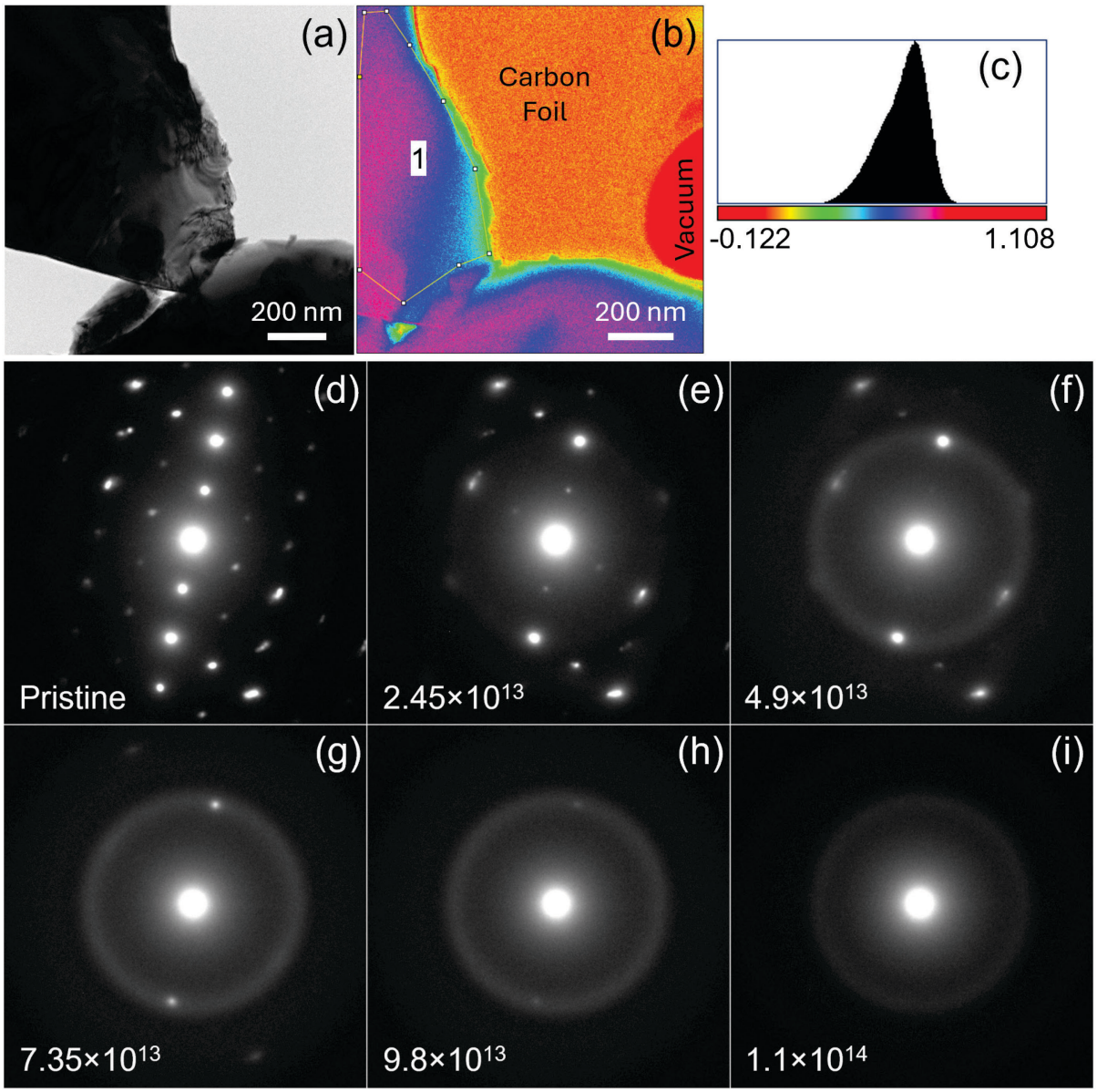

Figure 2. (a) Bright-field TEM image of HEO pyrochlore irradiated with 600 keV Xe ions at 298 K; (b) EF-TEM thickness map of sample; (c) pixel histogram for region labeled 1 in (b), which yields mean thickness value of 70 nm; (d) SAED pattern along [110] for unirradiated sample; (e) – (h) SAED patterns along [110] after irradiation with 600 keV Xe ions to different fluences at 298 K; (i) SAED pattern for amorphous state at a fluence of 1.1 $\times 10^{14}$ ions cm^{-2}.

electrons. The SAED pattern of the pristine (unirradiated specimen) is shown in Fig. 2 (d). SAED patterns taken at several increasing fluences during 600 keV Xe ion irradiation at 298 K are shown in Figs. 2 (e) – (i). Complete amorphization is observed at a fluence of 1.1 x 10^{14} ions/cm^2, as shown in Fig. 2 (i), and the

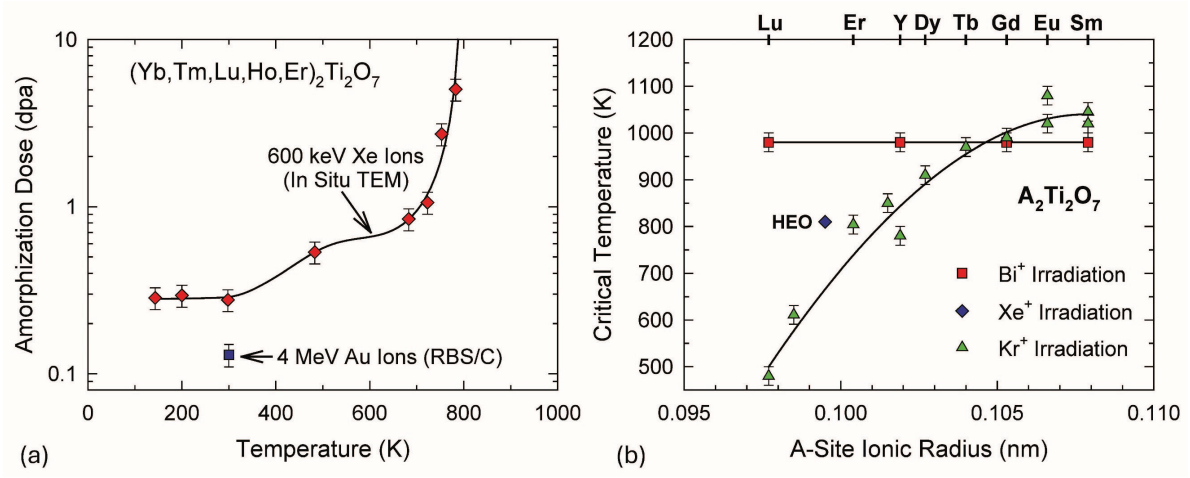

Figure 3. (a) Critical dose, D_c, for amorphization in the HEO pyrochlore after irradiation with 600 keV Xe ions at different temperatures; also included is the value of D_c previously determined in this HEO pyrochlore under irradiation with 4 MeV Au ions at room temperature [12]. (b) Critical temperature, T_c, for amorphization as a function of average A-site ionic radius for the HEO pyrochlore under 600 keV Xe ion irradiation, along with the values of T_c for several rare-earth titanate pyrochlores under 600 keV Bi ion irradiation [23] and 1.0 MeV Kr ion irradiation [27,28].

critical dose, D_c, for amorphization at 298 K is 0.27 dpa, as determined at a depth of 30 nm. The critical amorphization dose as a function of temperature is shown in Fig. 3 (a) for the in-situ TEM irradiation with 600 keV Xe ions; also included is the D_c value previously determined by RBS/C for this material due to irradiation with 4 MeV Au ions at room temperature, where D_c corresponds to the dose at which the RBS/C spectrum reaches the random level at the damage peak depth [12]. The in-situ critical dose at room temperature for the 600 keV Xe ions, 0.27 dpa, is about a factor of two larger than that previously determined by RBS/C for this material, 0.13 dpa, due to irradiation with 4 MeV Au ions [12], as well as larger than that determined for several simple rare-earth titanate pyrochlores by RBS/C for Au ion irradiations, 0.14 ± 0.01 dpa [24,25,26] and by in-situ TEM irradiation with 600 keV Bi ions, 0.18 ± 0.01 dpa [23]. However, the D_c value for the 600 keV Xe ions at room temperature is consistent with those values determined in other HEO pyrochlore compositions, 0.26 and 0.27 dpa [15,16] by in-situ TEM irradiation with 800 keV Kr ions. In contrast, similar in-situ studies on simple rare-earth titanate pyrochlores using 1 MeV Kr ions show a factor of three wider range of D_c values, 0.27 – 0.55 dpa [27]. In the case of single crystal $(Yb_{0.2}Tb_{0.2}Gd_{0.2}Dy_{0.2}Er_{0.2})_2Ti_2O_7$ pyrochlore irradiated at room temperature with 23 MeV Ni ions, the critical amorphization dose is 2.5 dpa [13], an order of magnitude higher than any other HEO or

Table 1. Critical dose, D_c, for amorphization determined for the HEO pyrochlore composition in this study, other HEO pyrochlore compositions, and related single-component rare-earth titanate pyrochlores under different irradiation conditions.

Composition	Irradiating Ion	D_c (dpa)	Characterization	Reference
$(Yb_{0.2}Tm_{0.2}Lu_{0.2}Ho_{0.2}Er_{0.2})_2Ti_2O_7$	4 MeV Au^+	0.13	RBS/C	[12]
$Gd_2Ti_2O_7$, $Sm_2Ti_2O_7$, $Ho_2Ti_2O_7$	1 - 4 MeV Au^+	0.14 ± 0.01	RBS/C	[24,25,26]
$(Yb_{0.2}Tm_{0.2}Lu_{0.2}Ho_{0.2}Er_{0.2})_2Ti_2O_7$	600 keV Xe^+	0.28	In-Situ TEM	This study
$(Lu_{0.25}Y_{0.25}Eu_{0.25}Gd_{0.25})_2Ti_2O_7$	800 keV Kr^+	0.26	In-Situ TEM	[15]
$(Lu_{0.2}Y_{0.2}Gd_{0.2}Eu_{0.2}Sm_{0.2})_2Ti_2O_7$	800 keV Kr^+	0.27 dpa	In-Situ TEM	[16]
$Y_2Ti_2O_7$, $Lu_2Ti_2O_7$, $Gd_2Ti_2O_7$, $Sm_2Ti_2O_7$	600 keV Bi^+	0.18 ± 0.01	In-Situ TEM	[23]
$Yb_2Ti_2O_7$, $Lu_2Ti_2O_7$, $Ho_2Ti_2O_7$, $Er_2Ti_2O_7$	1 MeV Kr^+	0.25 – 0.55	In-Situ TEM	[27]
$(Yb_{0.2}Tb_{0.2}Gd_{0.2}Dy_{0.2}Er_{0.2})_2Ti_2O_7$	23 MeV Ni^+	2.5 dpa	Raman	[13]

simple rare-earth titanate pyrochlore. A summary of all these critical doses for amorphization is presented in Table 1.

Based on the data in Figure 3(a), the critical temperature, T_c, for amorphization in the HEO pyrochlore in this study is determined to be 800 K under 600 keV Xe ion irradiations. Irradiation of this HEO pyrochlore with 600 keV Xe ions at 883 K resulted in only a weak halo in the SAED pattern at a dose of 37 dpa, indicating a partial amorphous state, and irradiation at 983 K and 1073 K at doses up to 60 dpa indicates no evidence for amorphization. In simple rare-earth titanate pyrochlores, the value of T_c tends to scale with the ionic radius of the A-site cation [27] but exhibits a strong dependence on the mass of the incident ions [28], as shown in Fig. 3(b). In the case of the HEO pyrochlore, the A-site ionic radius is assumed to be the average of the ionic radii for the rare-earth elements on the A-site, with a value of 0.0995 nm. The value of T_c, 800 K, for the HEO pyrochlore is less than that determined by in-situ TEM, 1000 K, for several simple rare-earth titanate pyrochlores irradiated with 600 keV Bi ions [23], as shown in Fig 3(b). In other simple rare-earth titanate pyrochlores irradiated with 1 MeV Kr ions, the critical temperatures for amorphization range from 480 K to 1100 K [27,28], depending on the ionic radius of the rare-earth cation, as shown in Fig. 3(b).

Discussion

The critical dose, D_c, for amorphization at room temperature in $(Yb_{0.2}Tm_{0.2}Lu_{0.2}Ho_{0.2}Er_{0.2})_2Ti_2O_7$ under 600 keV Xe ion irradiation in the present study is comparable to that measured in other HEO titanate pyrochlores at room temperature under similar in-situ TEM irradiation with 800 keV Kr ion irradiation, but less than that determined previously in the same material by RBS/C (Table 1). This dependence of D_c on mass of the incident ion has been previously observed in simple titanate pyrochlores, as shown in Table 1 for Au and Bi ion irradiations versus 1 MeV Kr ion irradiations, as well as in other ceramic materials [29]. This ion mass dependence has been attributed primarily to the efficiency of dynamic ionization-induced recovery along the ion trajectory that affects damage production and accumulation; it is related to the ratio, S_e/S_n, of electronic energy loss to nuclear energy loss for the different ions [10,29], which varies from about 0.25 for the Au and Bi ions to about 1.2 for 1 MeV Kr ions in the simple rare-earth titanate pyrochlores. This is supported by the much higher value of D_c (2.5 dpa) reported for $(Yb_{0.2}Tb_{0.2}Gd_{0.2}Dy_{0.2}Er_{0.2})_2Ti_2O_7$ under irradiation with 23 MeV Ni ions, where the ratio, S_e/S_n, is on the order of 100 at a depth of 100 nm. Although defect mobility is often minimal in these pyrochlores at room temperature, as supported by the near temperature independence of D_c at room temperature, as shown in Fig. 3 and reported for other simple titanate pyrochlores [23,27], defect recovery at the surfaces of the thin regions characterized in the in-situ TEM studies could also play a role in the higher values of D_c observed. This is consistent with the higher values of D_c (up to a factor of 2.3) reported for simple rare-earth titanate pyrochlores under in-situ TEM irradiation with 1 MeV Kr ions compared to the D_c values determined by cross-sectional TEM of similar single crystal pyrochlores irradiated with 1 MeV Kr ions [30]; however, the S_e/S_n ratio is significantly lower (~0.2) for the cross-sectional TEM determination of D_c as compared to 1.2 for the in-situ TEM determination, which further promotes the S_e/S_n dependence. In general, D_c for $(Yb_{0.2}Tm_{0.2}Lu_{0.2}Ho_{0.2}Er_{0.2})_2Ti_2O_7$ in this study does not indicate any significant increase or decrease in radiation tolerance relative to other HEO or simple titanate pyrochlores under similar irradiation conditions.

The HEO pyrochlore in this study consists of a random distribution of rare-earth cations on the A-site, and its radiation response may be representative of a mixture of simple rare-earth titanate pyrochlores having relevant A-site compositions. This seems to be the case for the critical dose for amorphization (Table 1) and is even more so for the critical temperature. The rare-earth cations on the HEO pyrochlore A-site all have ionic radii less than 0.1015 nm, with an average ionic radius of 0.0995 nm. As shown in Fig. 3(b), this average ionic radius positions the HEO pyrochlore in the lower range of A-site ionic radii, where the T_c exhibits a dependence on the mass of the incident ion for simple rare-earth titanates, and the value of T_c for the HEO pyrochlore for 600 keV Xe ion irradiation is between the values for 1 MeV Kr ions and 600 keV Bi ions, as expected [28,29]. This shift in critical temperature with ion mass in other pyrochlores and ceramics has been attributed to the effectiveness of dynamic ionization-induced recovery relative to damage

production along the ion trajectory that varies with composition, and models of this behavior in other materials indicate a dependence on the ratio S_e/S_n of the incident ions [10,29]. In the case of smaller ionic radii on the A-site (< 0.104 nm), including the HEO pyrochlore, T_c increases with increasing ion mass for a given composition; however, a correlation for variations in composition in the simple rare-earth titanate pyrochlores has yet to be developed due to limited data. Based on the models of this behavior, the temperature dependence of amorphization is independent of dose rate for this range of ionic radii and depends primarily on the ratio of ionization-induced recovery rate to damage production rate. For the case of larger A-site ionic radii (> 0.104 nm), the values of T_c converge. For these compositions, the thermal recovery rates are dominant and the kinetics of amorphization are dependent on dose-rate. As a result, T_c is defined by the condition where the thermal recover rate equals the damage production rate. Furthermore, the slight scatter in values of T_c at the higher values of ionic radii in Fig. 3(b) is most likely the result of different dose rates in each study. Clearly, additional irradiations of other HEO titanate pyrochlores having rare-earths on the A-site with larger ionic radii, as well as simple rare-earth titanate pyrochlores, are needed to fully interpret the T_c behavior under irradiation with 600 keV Xe ions, and such irradiations are planned.

Conclusions

The irradiation-induced amorphization of the HEO pyrochlore $(Yb_{0.2}Tm_{0.2}Lu_{0.2}Ho_{0.2}Er_{0.2})_2Ti_2O_7$ has been investigated by in-situ TEM under irradiation with 600 keV Xe ions over a range of temperatures. The critical dose for amorphization increases with temperature but is about a factor of two higher at 300 K than that previously determined under irradiation with 4 MeV Au ions. This difference is consistent with that observed in other HEO pyrochlores and related simple rare-earth titanate pyrochlores under different irradiation conditions, where the critical dose increases with decreasing mass of the incident ion. The critical temperature for amorphization in this HEO pyrochlore is 800 K under irradiation with 600 keV Xe ions. While the critical temperature for amorphization has not yet been reported for other HEO pyrochlore compositions, the critical temperature determined here is less than that determined for related rare-earth titanate pyrochlores under irradiation with 600 keV Bi ions but generally higher than those measured in related simple titanate pyrochlores under 1 MeV Kr ion irradiation. Additional studies on related simple titanate pyrochlores under 600 keV Xe irradiations are needed to better understand the role of the different A-site cations in the HEO pyrochlore on critical temperature. Further studies on the properties of amorphous HEO pyrochlores are needed, as are studies on the temperature dependence of amorphization in other HEO pyrochlore compositions.

Acknowledgements

The in-situ experiments were carried out at the MIAMI Irradiation Facility, which is part of the UK National Ion-Beam Centre (UKNIBC) funded by the Engineering and Physical Sciences Research Council (EPSRC)

of the UK. This research was supported in part by the National Science Foundation under Grant No. DMR-2104228. Y. Zhang acknowledges the support from Canada Excellence Research Chair Program. A. H. Mir is thankful to the EPSRC of the UK for funding support under Grant Number EP/T012811/1.

Author Contributions

William J. Weber: conceptualization, formal analysis, writing – original draft, writing – review & editing, visualization, funding acquisition. Candice Kinsler-Fedon: writing – review & editing. Veerle Keppens: writing – review & editing. Yanwen Zhang: writing – review & editing. Anamul H. Mir: conceptualization, methodology, investigation, formal analysis, writing – review & editing, visualization.

Funding

This work was supported in part by the National Science Foundation (Grant Number DMR-2104228). Y. Zhang was supported by the Canada Excellence Research Chairs, Government of Canada. A. H. Mir was supported by the Engineering and Physical Sciences Research Council of the UK (Grant Number EP/T012811/1).

Data availability

The data that support the findings of this study are available upon reasonable request.

Conflict of Interest

The authors have no conflicts of interest to declare that are relevant to the content of this article.

References

1. A. Sarkar, Q. Wang, A. Schiele, M.R. Chellali, S. S. Bhattacharya, D. Wang, T. Brezesinski, H. Hahn, L. Velasco, B. Breitung, High-Entropy Oxides: Fundamental Aspects and Electrochemical Properties. Adv. Mater. 31, 1806236 (2019). https://doi.org/10.1088/2515-7639/ad2ec5
2. T.Z. Ward, R. Wilkerson, B.L. Musicó, A. Foley, M. Brahlek, W.J. Weber, K.E. Sickafus, A. Mazza, High entropy ceramics for applications in extreme environments. J. Physics: Materials **7**, 021001 (2024). https://doi.org/10.1088/2515-7639/ad2ec5
3. F. Li, L. Zhou, J.X. Liu, Y. Liang, G.J. Zhang, High-entropy pyrochlores with low thermal conductivity for thermal barrier coating materials. J. Adv. Ceram. **8**, 576‑582 (2019). https://doi.org/10.1007/s40145-019-0342-4
4. C. Kinsler-Fedon, Q. Zheng, Q. Huang, E.S. Choi, J. Yan, H. Zhou, D. Mandrus, V. Keppens, Synthesis, characterization, and single-crystal growth of a high-entropy rare-earth pyrochlore oxide. Phys. Rev. Mater. **4**, 104411 (2020). https://doi.org/10.1103/PhysRevMaterials.4.104411
5. F. Vayer, C. Decorse, D. Bérardan D. Dragoe, N. Dragoe, Investigation of the chemical versatility in high-entropy pyrochlores. J. Amer. Ceram. Soc. **106**, 2601-2621 (2023). https://doi.org/10.1111/jace.18922

6. G. Karthick, L. Raman, B.S. Murty, Phase evolution and mechanical properties of novel nanocrystalline $Y_2(TiZrHfMoV)_2O_7$ high entropy pyrochlore. J. Mater. Sci. Technol. **82**, 214–226 (2021). https://doi.org/10.1016/j.jmst.2020.12.025
7. Z. Wang, C. Zhu, H. Wang, M. Wang, C. Liu, D. Yang, Y. Li, Preparation and irradiation stability of $A_2B_2O_7$ pyrochlore high-entropy ceramic for immobilization of high-level nuclear waste. J. Nucl. Mater. **574**, 154212 (2023). https://doi.org/10.1016/j.jnucmat.2022.154212
8. Y. Wang, Y.-J. Jin, Z.-Y. Ding, G. Cao, Z.-G. Liu, T. Wei, J.-H. Ouyang, Y.-M. Wang, Y.-J. Wang, Microstructure and electrical properties of new high-entropy rare-earth zirconates. J. Alloys Compd. **906**, 164331 (2022). https://doi.org/10.1016/j.jallcom.2022.164331
9. Y. Li, Y. Lei, H. Xiao, S. Zhao, Y. Wang, Z. Cao, J. Zhang, J. Wang, G. Lu, L. Cao, C. Wang, Different mechanisms of A-site and B-site high entropy effect on radiation tolerance of pyrochlores. J. Mater. Sci. Technol. **191**, 250–258 (2024). https://doi.org/10.1016/j.jmst.2024.02.002
10. Y. Zhang, W.J. Weber, Chapter 7: Defect Accumulation, Amorphization and Nanostructure Modification of Ceramics, in Ion Beam Modification of Solids – Ion-Solid Interaction and Radiation Damage, ed. by W. Wesch, E. Wendler (Springer, Switzerland, 2016), pp. 287-318. https://doi.org/10.1007/978-3-319-33561-2_7
11. L. Zhou, F. Li, J-X. Liu, S-K. Sun, Y. Liang, G-J. Zhang, High-entropy $A_2B_2O_7$-type oxide ceramics: A potential immobilising matrix for high-level radioactive waste. J. Hazard. Mater. **415**, 125596 (2021). https://doi.org/10.1016/j.jhazmat.2021.125596
12. C. Kinsler-Fedon, L. Nuckols, C.T. Nelson, Z. Qi, Q. Huang, D. Mandrus, Y. Zhang, W.J. Weber, V. Keppens, Effects of Au^{2+} irradiation induced damage in a high-entropy pyrochlore single crystal. Scr. Mater. 220, 114916 (2022). https://doi.org/10.1016/j.scriptamat.2022.114916
13. C. Kinsler-Fedon, Synthesis and Property Characterization of Rare-Earth High-Entropy Oxides with Pyrochlore-Type Structures. PhD diss., University of Tennessee, 2022. https://trace.tennessee.edu/utk_graddiss/7182
14. H. Guo, K. Zhang, Y. Li, Heavy-ion irradiation effects of high-entropy $A_2Ti_2O_7$ pyrochlore with multi-elements at a site. Ceram. Int. **50**, 21859–21868 (2024). https://doi.org/10.1016/j.ceramint.2024.03.298
15. H. Wang, C. Zhu, C. He, D. Yang, Y. Li, DFT+U study and in-situ TEM investigation of high-entropy titanate pyrochlore $(Lu_{0.25}Y_{0.25}Eu_{0.25}Gd_{0.25})_2Ti_2O_7$. J. Eur. Ceram. Soc. **42**, 7546–7552 (2022). https://doi.org/10.1016/j.jeurceramsoc.2022.09.028
16. H. Wang, C. Zhu, Z. Wang, M. Wang, Y. Li, Mechanical property and irradiation resistance of high entropy pyrochlore $(Sm_{0.2}Eu_{0.2}Gd_{0.2}Y_{0.2}Lu_{0.2})_2Ti_2O_7$. Nucl. Instrum. Meth. B **533**, 17–22 (2022). https://doi.org/10.1016/j.nimb.2022.10.011
17. G. Greaves, A.H. Mir, R.W. Harrison, M.A. Tunes, S.E. Donnelly, J.A. Hinks, New Microscope and Ion Accelerators for Materials Investigations (MIAMI-2) system at the University of Huddersfield. Nucl. Instrum. Meth. A **931**, 37–43 (2019). https://doi.org/10.1016/j.nima.2019.03.074
18. H. Shinotsuka, S. Tanuma, C.J. Powell, D.R. Penn, Calculations of electron inelastic mean free paths. XII. Data for 42 inorganic compounds over the 50eV to 200keV range with the full Penn algorithm. Surf. Interface Anal. **51**, 427–457(2018). https://doi.org/10.1002/sia.6598
19. A.H. Mir, N.C. Hyatt, S.E. Donnelly, An in-situ TEM study into the role of disorder, temperature and ballistic collisions on the accumulation of helium bubbles and voids in glass-ceramic composites. J. Nucl. Mater. **548**, 152836 (2021). https://doi.org/10.1016/j.jnucmat.2021.152836
20. J. Schindelin, I. Arganda-Carreras, E. Frise, V. Kaynig, M. Longair, T. Pietzsch, S. Preibisch, C. Rueden, S. Saalfeld, B. Schmid, J.Y. Tinevez, D.J. White, V. Hartenstein, K. Eliceiri, P. Tomancak, A. Cardona, Fiji: An open-source platform for biological-image analysis. Nature Methods **9**, 676–682 (2012). https://doi.org/10.1038/nmeth.2019
21. J.F. Ziegler, M.D. Ziegler, J.P. Biersack, SRIM – The stopping and range of ions in matter (2010). Nucl. Instrum. Meth. B **268**, 1818–1823 (2010). https://doi.org/10.1016/j.nimb.2010.02.091

22. W.J. Weber, Y. Zhang, Predicting Damage Production in Monoatomic and Multi-elemental Targets using Stopping and Range of Ions in Matter Code: Challenges and Recommendations. Curr. Opin. Solid State Mater. Sci. **23**, 100757 (2019). https://doi.org/10.1016/j.cossms.2019.06.001
23. B.D. Begg, N.J. Hess, W.J. Weber, R. Devanathan, J.P. Icenhower, S. Thevuthasan, B.P. McGrail, Heavy-Ion Irradiation Effects on Structures and Acid Dissolution of Pyrochlores. J. Nucl. Mater. **288**, 208-216 (2001). https://doi.org/10.1016/S0022-3115(00)00708-X
24. Y. Zhang, W.J. Weber, V. Shutthanandan, R. Devanathan, S. Thevuthasan, G. Balakrishnan, D.M. Paul, Damage Evolution on Sm and O Sublattices in Au-Implanted Samarium Titanate Pyrochlore. J. Appl. Phys. **95**, 2866-2872 (2004). https://doi.org/10.1063/1.1644891
25. S. Moll, G. Sattonnay, L. Thomé, J. Jagielski, C. Decorse, P. Simon, I. Monnet, W.J. Weber, Irradiation damage in $Gd_2Ti_2O_7$ single crystals: Ballistic versus ionization processes. Phys. Rev. B **84**, 064115 (2011). https://dx.doi.org/10.1103/PhysRevB.84.064115
26. Y. Zhang, J. Jagielski, I.-T. Bae, X. Xiang, L. Thome, G. Balakrishnan, D.M. Paul, W. J. Weber, Damage Evolution in Au-Implanted $Ho_2Ti_2O_7$ Titanate Pyrochlore. Nucl. Instrum. Meth. B **268**, 3009-3013 (2010). https://dx.doi.org/10.1016/j.nimb.2010.05.029
27. J. Lian, J. Chen, L.M. Wang, R.C. Ewing, J.M. Farmer, L.A. Boatner, K.B. Helean, Radiation-induced amorphization of rare-earth titanate pyrochlores. Phys. Rev. B **68**, 134107 (2003). https://dx.doi.org/10.1103/PhysRevB.68.134107
28. R.C. Ewing, J. Lian, W.J. Weber, Nuclear waste disposal–pyrochlore (A2B2O7): Nuclear waste form for the immobilization of plutonium and "minor" actinides. J. Appl. Phys. 95, 5949-5971 (2004). https://dx.doi.org/10.1063/1.1707213
29. W.J. Weber, D.M. Duffy, L. Thomé, Y. Zhang, The role of electronic energy loss in ion beam modification of materials. Curr. Opin. Solid State Mater. Sci. **19**, 1-11 (2019). http://dx.doi.org/10.1016/j.cossms.2014.09.003
30. J. Lian, L.M. Wang, R.C. Ewing, L.A. Boatner, Ion beam implantation and cross-sectional TEM studies of lanthanide titanate pyrochlore single crystals. Nucl. Instrum. Meth. B **241**, 365-371 (2005). https://doi.org/10.1016/j.nimb.2005.07.043